Large magnetic anisotropy in canted antiferromagnetic Sr_2IrO_4 single crystals

Yunjeong Hong and Younjung Jo*
Department of Physics, Kyungpook National University, Daegu, 41566, Republic of Korea

Hwan Young Choi, Nara Lee, and Young Jai Choi
Department of Physics and IPAP, Yonsei University, Seoul, 04056, Republic of Korea

Woun Kang
Department of Physics, Ewha Womans University, Seoul, 03760, Republic of Korea
(Received 30 October 2015; revised manuscript received 11 February 2016; published 7 March 2016)

The magnetocrystalline contribution to magnetic anisotropy was studied in the canted antiferromagnetic state of layered Sr_2IrO_4 single crystals. We performed torque measurements in magnetic fields up to 9 T under various magnetic field orientations. The strong dependence of torque on the magnetic field revealed that the magnetic easy axis is along the in-plane direction and that the observed field-induced weak ferromagnetic order is attributed only to the in-plane component of the external magnetic field. The dependence of torque on the angle produces a twofold symmetric sawtoothlike shape. A simple model consisting of canted antiferromagnetic and magnetic induction terms showed good agreement with the measured torque. These results show that magnetic anisotropy is closely related to the anisotropy of the exchange between antiferromagnetic moments whose canting is mediated by the Dzyaloshinsky-Moriya interaction. Our study demonstrates that torque magnetometry can be extended to the investigation of the magnetic anisotropy of complex magnetic phases.

DOI: 10.1103/PhysRevB.93.094406

I. INTRODUCTION

Iridates represent one of the most studied families among strong spin-orbit-coupled materials. It has been realized that a strong relativistic spin-orbit coupling can drastically modify magnetic interactions such as the giant magnetoelastic effect [1] and can yield a far richer phase diagram for magnetic systems than those obtained from conventional models. In strong spin-orbit-coupled Sr_2IrO_4, a rotation of the IrO_6 octahedron of approximately 11° about the c axis and a distorted in-plane Ir-O-Ir bond angle are critical to a variety of magnetic phenomena such as spin canting from the a axis. The canting of the moments yields a nonzero net moment within a layer, which is ordered in the up-down-down-up spin pattern along the c axis. This magnetism can be interpreted based on the alignment of the effective total angular moment J_{eff}, where the canted J_{eff} is placed on the plane of the IrO_6 octahedron below $T_N = 230$ K [2–11].

Whereas the magnetic ground state has been investigated using several theoretical and experimental approaches, the magnetisms for fields applied along different crystallographic directions have not yet been thoroughly evaluated. In particular, it is not clear how the magnetic response of Sr_2IrO_4 to the out-of-plane magnetic field orientation ($H \parallel c$ axis) contributes to the magnetic anisotropy [8,10,12]. Experimentally, the anisotropic magnetoresistivity showed no apparent correlation to the magnetization when $H \parallel c$ axis [13]. The inelastic Raman scattering studies of Sr_2IrO_4 showed a weak magnetic field dependence of the spin-wave mode energy for $H \parallel c$ axis, which is consistent with electron-spin-resonance results [14].

Layered transition oxides exhibit intrinsic easy and hard directions of magnetization; that is, the energy required to magnetize a crystal depends on the direction of the applied field relative to the crystal axes. The two main sources of magnetic anisotropy are the magnetic dipolar interaction and the spin-orbit interaction. The dipolar interaction can be neglected in bulk crystals. The correlation between spin and orbital governed by lattice distortions mostly confines the orientation of the magnetization relative to the crystalline axes, which gives rise to magnetocrystalline anisotropy [15].

Measuring the anisotropic susceptibility and magnetization directly obtained from a superconducting quantum interference device (SQUID) or vibrating-sample magnetometer (VSM) is an accurate method of investigating macroscopic magnetic structure. However, there are some limitations, such as the difficulty of applying high magnetic fields and making minute angle adjustments. Torque magnetometry has been widely used to evaluate magnetic anisotropy in terms of the components of the magnetic susceptibility tensor $\vec{m}$ for fields $\vec{B}$ applied along different crystallographic directions, i.e., $\vec{\tau} = \vec{m} \times \vec{B}$. In a layered honeycomb Li_2IrO_3, the highly anisotropic spin exchange was studied. When the field is rotated to the ac plane, the torque directly indicates magnetic anisotropy on angles, i.e., $\tau(\theta) = \frac{(\chi_c - \chi_a)H^2 \sin(2\theta)}{2}$, where θ is the angle between the direction of magnetization and that of the external field [16]. In isovalent doped iron pnictides, electronic nematicity has also been researched using torque magnetometry, which is confirmed by the breaking of the structural symmetry [17]. In many epitaxial films, anisotropy energy [18], the dominant effect of anisotropy [19], and the energetically favored axis of the orientation of the magnetization [20] were investigated by changing the angles between the magnetization and the field direction.

In this study, we used torque magnetometry as a sensitive probe to investigate the macroscopic magnetic anisotropy in Sr_2IrO_4 single crystals. We measured the field $\tau(H)$ and angle dependences $\tau(\theta)$ of the magnetic torque in Sr_2IrO_4 single

*jophy@knu.ac.kr

crystals under a magnetic field greater than 1 T. In particular, this is the first observation of the angle dependence of canted antiferromagnetic ordering at high resolution, i.e., at as small as 1°. We found that $\tau(\theta)$ deviates from the simple $\sin(2\theta)$ behavior expected for conventional layered materials. As a result of fitting $\tau(\theta)$ to a model equation, we concluded that highly anisotropic magnetism in Sr_2IrO_4 is strongly related to the anisotropic exchange of canted antiferromagnetic (CAF) moments accompanying the change in lattice geometry.

II. EXPERIMENTAL DETAILS

Sr_2IrO_4 single crystals were synthesized using a flux method with $SrCl_2$ as the flux [21], and the crystallinity was confirmed using x-ray diffraction. Temperature- and magnetic- field-dependent magnetizations were measured using a SQUID (Quantum Design, Inc., San Diego, CA, USA). A Sr_2IrO_4 single crystal was mounted on a piezo cantilever with its crystallographic c axis perpendicular to the plane of the lever; the displacement was measured via changes in the resistance of the piezo lever [22]. The change in resistance, which is proportional to torque, was measured with a Wheatstone bridge using a physical property measurement system (PPMS; Quantum Design, Inc.), in which a rotator allowed the cantilever to change its orientation with respect to the direction of the applied field.

III. RESULTS AND DISCUSSION

Figure 1(a) shows the field dependence of the magnetization and magnetic torque at 5 K when the magnetic field is applied along the in-plane direction. We define the angle θ relative to the ab plane such that $\theta = 0°$ corresponds to fields aligned along the planar direction. A nonzero θ corresponds to a rotation of the field toward an out-of-plane direction of the sample [see the diagram in Fig. 2(c)]. As the strength of the magnetic field increases, magnetization gradually increases and saturates above a certain critical field $H_c = 0.25$ T [3], showing a small saturated magnetic moment of $0.05\mu_B$/f.u. This result is consistent with those of previous reports [4,21,23]. The same behavior is observed in the torque, whose slope changes near H_c, exhibiting hysteresis. The metamagnetic transition near H_c is attributed to a sudden flopping of each spin in the Ir ions over its inverse direction. The remanent net moments J_{eff}, which are the vector sum of the canted antiferromagnetic spins, align ferromagnetically, layer by layer, under applied magnetic fields.

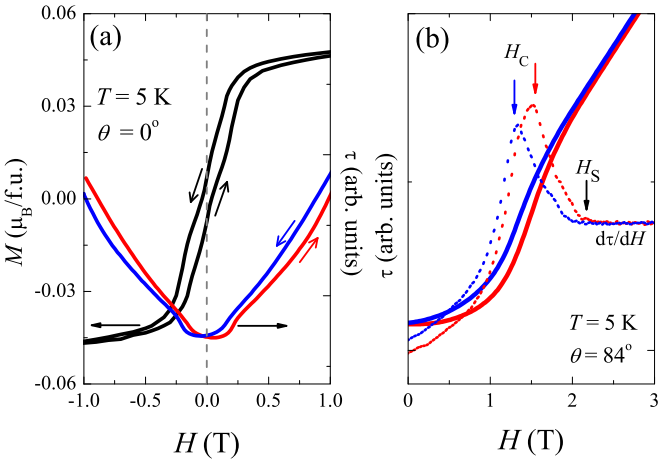

FIG. 1. (a) Magnetization and torque of the Sr_2IrO_4 crystal at $T = 5$ K when the magnetic field is applied along the in-plane direction. (b) Torque and differential torque at $\theta = 84°$ with the definition of weak ferromagnetic field H_c and saturation field H_s.

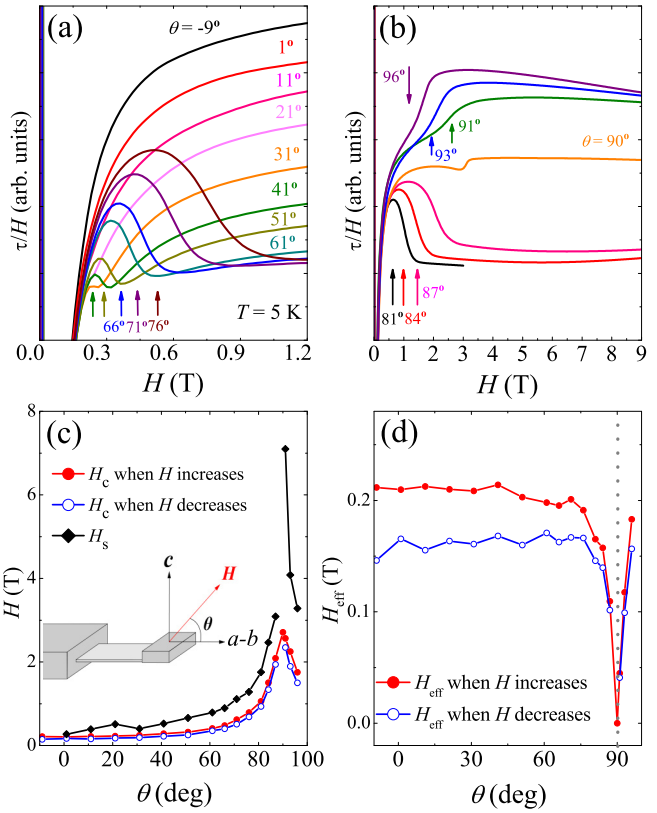

FIG. 2. (a) and (b) Field dependence of torque at 5 K for various angles. The arrows indicate the weak ferromagnetic transition fields H_c. (c) Angle dependence of the transition points at 5 K. Red and blue symbols indicate the transition points when the field is increased and decreased, respectively. The inset is a schematic plot of the piezo cantilever where the sample is mounted on the lever. The magnetic field is rotated with an angle θ from the in-plane direction of the sample. (d) Effective fields H_{eff} as a function of the angle θ, where the in-plane component of the critical point H_c is.

The magnetic moment of magnetically anisotropic materials will tend to align along the easy axis because it is the most energetically favorable direction of spontaneous magnetization. However, magnetic moments do not align exactly along the direction of the applied field but, instead, align at some angle θ. The details concerning the dependence of the magnetic response on the angle were studied using angle-resolved torque magnetometry. We defined two points, H_c and H_s, as the antiferromagnetic to weakly ferromagnetic spin-flop transition field and the magnetization saturation field, respectively. As shown in Fig. 1(b), these fields are clearly observed at an angle $\theta = 84°$ in the differential torque ($d\tau/dH$) for increasing and decreasing magnetic field sweeps. We observed that $d\tau/dH$ has a peak at H_c where $d\tau/dH$ has an inflection point, whereas the hysteresis disappears at H_s.

A significant angular dependence is observed in $\tau(H)/H$. In Figs. 2(a) and 2(b), $\tau(H)/H$ is plotted for selected angles below and above 80° at 5 K, respectively. All of the curves show an inflection point at H_c, as indicated by the arrows. H_c is slightly shifted to higher values with increasing angles. However, an abrupt increase in H_c can be observed near 90° in Fig. 2(b). When the magnetic field is applied along the c-axis direction ($\theta = 90°$), the torque responses to increasing and decreasing fields are quite different. A clear kink is observed at 3 T only for increasing fields; however, no kink is observed in the decreasing field sweep, and no saturation is observed below 9 T. When the angle θ is near 91°, the saturation field H_s is observed above 7 T. We show the values of H_c and H_s as a function of θ in Fig. 2(c). When the magnetic field is applied along the interplanar direction, Sr_2IrO_4 does not experience any metamagnetic transition, at least for applied fields up to 9 T. This behavior is well represented by the effective field H_{eff} shown in Fig. 2(d), where H_c is projected onto the crystal plane, i.e., $H_{eff} = H_c|\cos(\theta)|$. H_{eff} shows the critical field of 0.2 and 0.15 T for increasing and decreasing field at all angles except very near $\theta = 90°$. The difference of the H_{eff} values between increasing and decreasing fields is due to the hysteretic properties. This result implies that a realignment of J_{eff} follows only the in-plane component of the magnetic fields.

We also performed angle-dependent torque $\tau(\theta)$ measurements at fixed fields ranging from 1 to 7 T at 30 K [see Fig. 3(a)]. The $\tau(\theta)$ behavior of a Sr_2IrO_4 single crystal reveals a highly anisotropic susceptibility. The torque vanishes when the magnetic field is applied for $\theta = 0°$ and 90°, which indicates that the ab plane and c axis are both either easy or hard axes. We adjusted the torque to zero by rotating the sample to $\theta = 0°$. The stronger the magnetic field is, the larger the torque is, and a pronounced sawtoothlike dependence on the angle was detected. The twofold symmetric sawtoothlike signal is not usually observed in conventional metal oxides in which the torque sinusoidally depends on the angle. There are two requirements for determining whether the total magnetization can be mainly attributed to the CAF alignment: the amplitude of the torque should be proportional to the field strength, and the shape of $\tau(\theta)$ should be sawtoothlike [24–27]. A linear fit of the maximum amplitude of torque as a function of the magnetic field shows high reliability [Fig. 3(c)]. We adopted a simple model to analyze $\tau(\theta, H)$ as follows.

We assume that the magnetic field is rotated in a plane defined by both a direction along the basal plane and the interplanar c axis. The angle θ is defined with respect to the basal plane. The component of the saturated magnetization along the basal plane M_s is defined by the projection of the external field onto the basal plane, forming an angle α relative to the intersection between the basal plane and rotated plane. The magnetic torque τ is then developed in the rotated plane, where the magnetization component on the rotated plane M_c subtends an angle γ from the intersection. The torque is simply described by $\tau = M_c H \sin(\theta - \gamma)$ when the sample is perfectly aligned, i.e., $\theta_0 = 90°$ from the basal plane. However, there is always a misalignment of the positioning of the sample, and the rotated plane deviates from $\theta_0 = 90°$. We found that θ_0 is approximately 93°, which cannot be neglected. Using M_s instead of M_c is more intuitive, and therefore, we

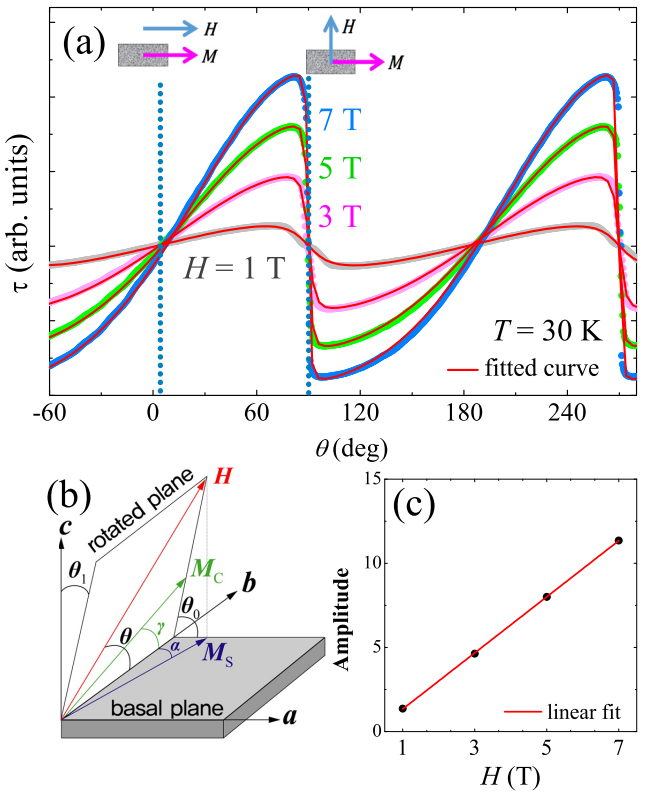

FIG. 3. (a) Angle dependence of the torque of Sr_2IrO_4 under various magnetic fields at $T = 30$ K. The solid red line fits the model, taking into account the canted antiferromagnetic and induced magnetization terms (see the text). (b) Schematic diagram of the relation between the basal plane and the rotated plane, including several parameters. (c) The amplitudes of torque change linearly with the applied magnetic fields.

define

$$M_c \sin\theta = M_s \sin\alpha \cos\theta_0, \tag{1}$$

where $\tan\alpha = \tan\theta\cos\theta_0$ and $\tan\gamma = \tan\alpha\cos\theta_0$. Using a trigonometric calculation, the torque induced by CAF alignment τ_{CAF} is expressed as

$$\tau_{CAF} = \frac{\cos(\theta)}{|\cos(\theta)|}\frac{M_s \sin(\theta)\sin^2\theta_0}{\sqrt{1+\tan^2(\theta)\cos^2\theta_0}}H. \tag{2}$$

To determine the total magnetization of Sr_2IrO_4, we assume that the CAF and induced magnetization (IM) terms are important; i.e., $M_{total} = M_{CAF} + M_{IM}$. Thus, the torque signal can be represented as $\tau(H) = A_{CAF}H + A_{IM}H^2$, where A_{CAF} and A_{IM} provide different responses to the direction of the applied magnetic field. The first term derives from the CAF moment in the basal plane with a contribution from the canting effect. The second term is the quantity of magnetization induced by the strong external magnetic field. The angle- and field-dependent torque $\tau(\theta, H)$ is then expressed by

$$\tau(\theta,H) = \frac{\cos(\theta+\theta_1)}{|\cos(\theta+\theta_1)|}\frac{B\sin(\theta+\theta_1)\sin^2\theta_0}{\sqrt{1+\tan^2(\theta+\theta_1)\cos^2\theta_0}}H + D\sin(2\theta+\theta_1)H^2 + F, \tag{3}$$

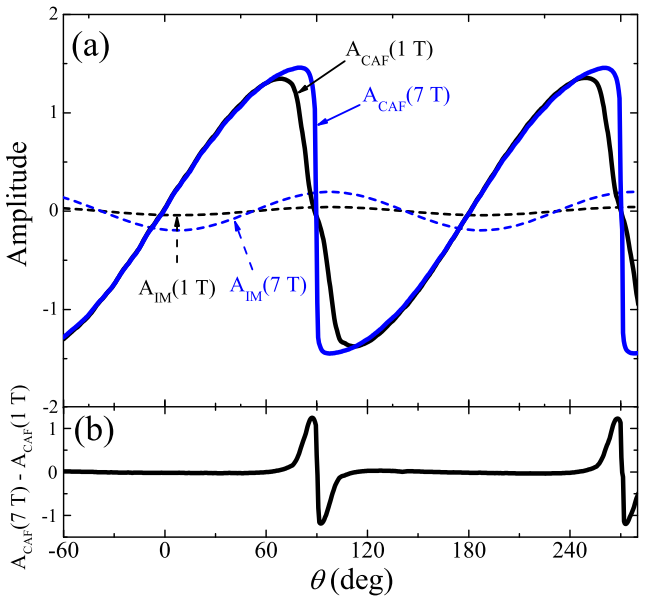

FIG. 4. (a) Angle dependence of the canted antiferromagnetic term (solid lines) and induced magnetization term (dashed lines) when fields of 1 T (black) and 7 T(blue) are applied. Both graphs are gained from fitting the graph to Eq. (3). (b) The graph of the subtraction of CAF terms, when fields of 7 and 1 T are applied, vs the angles.

where θ_1 is a correction variable for an initial orientation of the basal and rotated planes, F is an offset resistance of the piezo cantilever, and B and D are fitting parameters. B is the parasitic magnetic moment, which is the remanent moment from the CAF moments without external fields. D is the anisotropy between the in-plane and out-of-plane susceptibilities, i.e., $(\chi_{ab} - \chi_c)/2$. According to $\tau(H)$ for different angles in Fig. 2, it is proven that Sr_2IrO_4 is highly anisotropic between the in-plane direction and the out-of-plane direction. We can neglect the interplanar interactions, and thus, D represents only the in-plane susceptibility. Both B and D are intrinsic properties and are very slightly changed by the magnetic fields. Equation (3) accurately reproduces the observed data shown in Fig. 3(a), shown as solid red lines, which means that the CAF and IM terms can explain the macroscopic magnetic responses of Sr_2IrO_4 under a high applied magnetic field.

We estimated the anisotropic magnetism of Sr_2IrO_4 by comparing the amplitudes of A_{CAF} and A_{IM} at 1 and 7 T in Fig. 4 (a). Although both A_{CAF} and A_{IM} contribute to the magnetization, A_{CAF} (solid line) is greater than A_{IM} (dotted line), with an enhancement when $H = 7$ T. The conclusion is that the intrinsic canted antiferromagnetism is dominant and more important for determining the magnetic anisotropy. Figure 4(b) shows the deviation of A_{CAF} at 7 T from that at 1 T. The influences of A_{CAF} on the magnetic fields are consistent, except at approximately $\theta = 90^\circ$, where the magnetic field is applied along the out-of-plane direction of the crystal. This phenomenon clearly reflects that the two-dimensional antiferromagnetic correlation is crucial, whereas the magnetic interaction along the out-of-plane direction is not influential [9,28].

Our angle-resolved torque $\tau(\theta)$ shows that the CAF term has a major influence on the shape and amplitude of the torque. This result implies that a highly anisotropic magnetism in Sr_2IrO_4 is strongly related to the anisotropic exchange of CAF moments accompanying the change in lattice geometry. Furthermore, even under high magnetic fields above H_c, the magnetic anisotropy is prone to following the motion of the spin component rather than the spin-orbit coupled J_{eff} moments. Recent studies of Sr_2IrO_4 have already established that the canted magnetic moment is sensitive to the bond angle. A theoretical approach to implementing the Kitaev model in the magnetic structure of insulating Sr_2IrO_4 was recently developed [29]. Accounting for the rotations of the IrO_6 octahedra, the Hamiltonian contains isotropic, symmetric, and antisymmetric antiferromagnetic exchange couplings. Among these couplings, antisymmetric antiferromagnetic exchange coupling is found to be a dominant contributor to CAF ordering. This uncompensated antiferromagnetic exchange coupling can be ascribed to the Dzyaloshinsky-Moriya (DM) interaction. In the context of a DM interaction, tetragonal elongation along the c axis leads to octahedral rotation and bond-angle alteration between Ir-O-Ir. The bond length and bond angle are approximately 1.97 Å and 159°, respectively, and canted spin moments rigidly follow octahedral rotation [7,29]. This is significantly different for La_2CuO_4, which has crystal and magnetic structures equivalent to those of Sr_2IrO_4 [23]. As the IrO_6 octahedra rotate with the spins, the application of the $H \parallel ab$ plane induces the rotation of the IrO_6 octahedra, which, in turn, changes the bond angle. However, the application of the $H \parallel c$ axis has very little effect on the spin reconfiguration. We conclude that antiferromagnetic exchange coupling makes a substantial contribution to magnetic anisotropy in Sr_2IrO_4. Our result is quite significant in terms of the ability of J_{eff} states to explain bulk magnetism.

IV. CONCLUSIONS

In this study, we investigated the magnetism of the strongly spin-orbit-coupled Sr_2IrO_4 single crystals via torque magnetometry under high applied magnetic fields. Previously, magnetization and magnetic susceptibility results limited our ability to understand the anisotropic alignment of the J_{eff} moments and to predict the effects of strong magnetic fields. We measured the angle and the field dependence of torque using a piezo cantilever torque magnetometer and the rotator option of a PPMS. From the field-dependent experiment for different angles, we concluded that only the in-plane component of the magnetic field stimulates the weak ferromagnetic ordering of the Sr_2IrO_4 crystal. The c axis is the hard axis because extremely high fields are required to orient the moments along the c-axis direction. For the angle-dependent experiment, we compared the results with fitted torque curves, considering the CAF and IM terms. We determined that the CAF order is crucial for determining the magnetic anisotropy, which is closely related to the anisotropy of the antiferromagnetic exchange coupling mediated by the DM interaction. To summarize, a clear macroscopic two-dimensional magnetic structure exists under high magnetic fields.

ACKNOWLEDGMENTS

We wish to thank L. Balicas and J. S. Kim for their invaluable input. This work was supported by the National Research Fund (NRF; NRF-2013R1A1A2063904, NRF-2013R1A1A2058155, NRF-2014S1A2A2028481, and NRF-2015R1C1A1A02037744) and the Korean Basic Science Institute (KBSI) and partially by the Yonsei University Future-leading Research Initiative of 2014 (2014-22-0123). W.K. is supported by the NRF grants funded by the Korea Government (MSIP) (Grants No. 2015-001948 and No. 2010-00453).

[1] S. Chikara, O. Korneta, W. P. Crummett, L. E. DeLong, P. Schlottmann, and G. Cao, Phys. Rev. B **80**, 140407 (2009).
[2] Q. Huang, J. Soubeyroux, O. Chmaissem, I. N. Sora, A. Santoro, R. Cava, J. Krajewski, and W. Peck, J. Solid State Chem. **112**, 355 (1994).
[3] B. Kim, H. Ohsumi, T. Komesu, S. Sakai, T. Morita, H. Takagi, and T. Arima, Science **323**, 1329 (2009).
[4] M. K. Crawford, M. A. Subramanian, R. L. Harlow, J. A. Fernandez-Baca, Z. R. Wang, and D. C. Johnston, Phys. Rev. B **49**, 9198 (1994).
[5] I. Franke, P. J. Baker, S. J. Blundell, T. Lancaster, W. Hayes, F. L. Pratt, and G. Cao, Phys. Rev. B **83**, 094416 (2011).
[6] C. Dhital, T. Hogan, Z. Yamani, C. de la Cruz, X. Chen, S. Khadka, Z. Ren, and S. D. Wilson, Phys. Rev. B **87**, 144405 (2013).
[7] S. Boseggia, H. C. Walker, J. Vale, R. Springell, Z. Feng, R. S. Perry, M. Moretti Sala, H. M. Rønnow, S. P. Collins, and D. F. McMorrow, J. Phys. Condens. Matter **25**, 422202 (2013).
[8] S. Boseggia, R. Springell, H. C. Walker, H. M. Rønnow, Ch. Rüegg, H. Okabe, M. Isobe, R. S. Perry, S. P. Collins, and D. F. McMorrow, Phys. Rev. Lett. **110**, 117207 (2013).
[9] F. Ye, S. Chi, B. C. Chakoumakos, J. A. Fernandez-Baca, T. Qi, and G. Cao, Phys. Rev. B **87**, 140406 (2013).
[10] M. Ge, T. F. Qi, O. B. Korneta,, D. E. De Long, P. Schlottmann, W. P. Crummett, and G. Cao, Phys. Rev. B **84**, 100402 (2011).
[11] O. B. Korneta, T. Qi, S. Chikara, S. Parkin, L. E. De Long, P. Schlottmann, and G. Cao, Phys. Rev. B **82**, 115117 (2010).
[12] Y. Gim, A. Sethi, Q. Zhao, J. F. Mitchell, G. Cao, and S. L. Cooper, Phys. Rev. B **93**, 024405 (2016).
[13] C. Wang, H. Seinige, G. Cao, J.-S. Zhou, J. B. Goodenough, and M. Tsoi, Phys. Rev. X **4**, 041034 (2014).
[14] S. Bahr, A. Alfonsov, G. Jackeli, G. Khaliullin, A. Matsumoto, T. Takayama, H. Takagi, B. Büchner, and V. Kataev, Phys. Rev. B **89**, 180401(R) (2014).
[15] G. Bertotti, *Hysteresis in Magnetism: For Physicists, Materials Scientists, and Engineers* (Academic, San Diego, 1998).
[16] K. A. Modic, T. E. Smidt, I. Kimchi, N. P. Breznay, A. Biffin, S. Choi, R. D. Johnson, R. Coldea, P. Watkins-Curry, G. T. McCandless, J. Y. Chan, F. Gandara, Z. Islam, A. Vishwanath, A. Shekhter, R. D. McDonald, and J. G. Analytis, Nat. Commun. **5**, 4203 (2014).
[17] S. Kasahara, H. J. Shi, K. Hashimoto, S. Tonegawa, Y. Mizukami, T. Shibauchi, K. Sugimoto, T. Fukuda, T. Terashima, A. H. Nevidomskyy, and Y. Matsuda, Nature (London) **486**, 382 (2012).
[18] C. M. Williams, J. J. Krebs, F. J. Rachford, G. A. Prinz, and A. Chaiken, J. Magn. Magn. Mater. **110**, 61 (1992).
[19] A. Lisfi, C. M. Williams, L. T. Nguyen, J. C. Lodder, A. Coleman, H. Corcoran, A. Johnson, P. Chang, A. Kumar, and W. Morgan, Phys. Rev. B **76**, 054405 (2007).
[20] G. H. O. Daalderop, P. J. Kelly, and F. J. A. den Broeder, Phys. Rev. Lett. **68**, 682 (1992).
[21] G. Cao, J. Bolivar, S. McCall, J. E. Crow, and R. P. Guertin, Phys. Rev. B **57**, R11039 (1998).
[22] J. Brugger, M. Despont, C. Rossel, H. Rothuizen, P. Vettiger, and M. Willemin, Sens. Actuators A **73**, 235 (1999).
[23] I. N. Bhatti, R. Rawat, A. Banerjee, and A. Pramanik, J. Phys. Condens. Matter **27**, 016005 (2015).
[24] F. Martín-Hernández and A. M. Hirt, Geophys. J. Int. **157**, 117 (2004).
[25] H. Porath and F. H. Chamalaun, Pure Appl. Geophys. **64**, 81 (1966).
[26] E. C. Ferré, F. Martn-Hernández, C. Teyssier, and M. Jackson, Geophys. J. Int. **157**, 1119 (2004).
[27] F. Martin-Hernandez and A. M. Hirt, Geochem. Geophys. Geosyst. **14**, 4444 (2013).
[28] S. Fujiyama, H. Ohsumi, T. Komesu, J. Matsuno, B. J. Kim, M. Takata, T. Arima, and H. Takagi, Phys. Rev. Lett. **108**, 247212 (2012).
[29] G. Jackeli and G. Khaliullin, Phys. Rev. Lett. **102**, 017205 (2009).